Original Article

Age- and gender-related normal references of right ventricular strain values by tissue tracking cardiac magnetic resonance: results from a Chinese population

Ting Liu[#], Congcong Wang[#], Shu Li, Yu Zhao, Peiling Li

Department of Radiology, The First Affiliated Hospital of China Medical University, Shenyang 110001, China

[#]These authors contributed equally to this work.

Correspondence to: Peiling Li. Department of Radiology, the First Affiliated Hospital of China Medical University, Shenyang 110001, China. Email: lipeilingcmu@163.com.

Background: Myocardial deformation is a sensitive marker for sub-clinical myocardial dysfunction and carries independent prognostic significance across a broad range of cardiovascular diseases. Reproducible and repeatable assessment of right ventricular (RV) function is vital for monitoring congenital and acquired heart diseases. The purpose of this study was to determine the normal references of RV strain and strain rate values using tissue tracking cardiac magnetic resonance imaging (MRI).

Methods: A cohort of 120 normal human subjects from each decade of life between 20 and 70 without cardiac diseases were enrolled in this study. Retrospectively, electrocardiogram (ECG) gating cardiac MRI imaging was performed at 3.0T with balanced steady-state free precession (bSSFP) imaging. RV global and segmental myocardial strains were analyzed by tissue tracking by two experienced observers.

Results: The global peak longitudinal strain (GLS) and global peak radial strain (GRS) was –24.3±4.7 and 23.0±8.5 respectively. For the peak circumferential strains (GCS), the values for global, basal, mid-cavity, and apical segments were –13.3±4.1, –13.1±4.0, –12.5±4.7, and –15.9±5.8, respectively. There were significant gender differences in peak GRS (P=0.009) and at the base (P=0.017) and the mid-cavity (P=0.011) with greater deformation in females than in males. There were also significant age differences in GRS (P<0.001), GCS for basal (P<0.001), and mid-cavity segments (P=0.037). On Bland-Altman analysis, peak GLS and GRS had the best intra-observer agreement (mean bias, –0.13±0.51; 95% CI, –1.13–0.87) and inter-observer (mean bias, 0.054±0.31; 95% CI, –0.55–0.66) agreement, respectively.

Conclusions: Normal values of RV deformation for healthy individuals using tissue tracking cardiac magnetic resonance (CMR-TT) provided good RV peak strain reproducibility. There was a significant correlation between RV strain or strain rate parameters with either age or sex.

Keywords: Cardiac magnetic resonance (CMR); tissue tracing; right ventricular (RV); myocardial strain; strain rate

Submitted Apr 23, 2019. Accepted for publication Aug 20, 2019.
doi: 10.21037/qims.2019.08.13
View this article at: http://dx.doi.org/10.21037/qims.2019.08.13

Introduction

In recent years, right ventricular (RV) function has been increasingly recognized for its prognostic role in a wide variety of cardiovascular and pulmonary diseases. However, due to the complex structure of the RV, dense myocardial trabeculae, the ventricular anatomical structure behind the sternum and complex movement, and the evaluation methods for RV function are greatly limited (1,2). Although widely used in clinical practice, transthoracic echocardiography (TTE) lacks standard reference and relies

on manipulations (3-5). Cardiac magnetic resonance (CMR), as a non-invasive imaging technology that produces three-dimensional detailed anatomical images without the use of ionizing radiation can overcome some of the limitations of echocardiography and can visualize the entire RV in a repeatable manner.

Although RV ejection fraction (EF) resulting from CMR is often used as a reference of RV function in clinical routine, more and more studies have shown that myocardial strain and strain rate have a significant clinical value for the evaluation of regional and global myocardial function, especially for the early detection of systolic ventricular dysfunction before EF reduction (3-8). The CMR technique to obtain myocardial strain can provide sensitive indication for the early detection of cardiovascular dysfunction (6-8). RV strain and strain rate values were initially evaluated using myocardial tagging technology (9). However, the laborious post-processing to extract and track the tagged lines on myocardium remains the major drawback of this tagging technology (10).

More recently, CMR cine image-based tissue tracking technology (CMR-TT) has allowed for a rapid and reliable quantification of myocardial deformation, with the advantage of high image quality unhindered by the availability of an adequate acoustic window (8-10). Normal ranges have been reported for left ventricular (LV) strain and strain rates using CMR-TT (8). Data for the right heart based on CMR-TT required to ensure clinical utility are limited. Therefore, the purpose of this study was to analyze the normal parameters of RV myocardial strain and strain rate in healthy subjects using CMR-TT and to evaluate the range of normal parameters and their correlation.

Methods

Study population

A total of 120 healthy volunteers, 12 men and 12 women in each of the 5 age deciles from 20 to 70 years, were included. All subjects received a CMR scan in our center with informed consent. Self-report history was taken to exclude subjects with chest pain, breathlessness or other cardiac symptoms, and those with a history of hypertension, diabetes, dyslipidemia, or any cardiovascular, renal, hepatic, hematological and systemic inflammatory disease. Clinical examination was performed, including office blood pressure (normal b140/90 mmHg). Blood samples were taken to confirm normal range full blood count, serum electrolytes, and random glucose. All subjects had a normal resting 12 lead ECG and either negative exercise stress echocardiography or exercise ECG. Demographic data, excluding ethnicity, were collected, and informed consent was obtained from each patient.

CMR acquisition

All subjects underwent cine CMR on 3T (Vero, Siemens, Germany) CMR scanners. The scanners used a 32-channelcardiac coil and a balanced steady-state free precession (b-SSFP) sequence with ECG gating and gated respiratory control to obtain cine CMR images, comprising a stack of contiguous short-axis slices covering the entire RV from base to apex; the long axis four-chamber slice images were also obtained. The scan was performed using the following parameters: FOV, 286 mm × 340 mm; matrix, 216×256; TR, 3.40 ms; echo time (TE), 1.70 ms; time resolution, 40 ms; slice thickness, 8 mm; 25 phases per cardiac cycle were generated resulting in a mean temporal resolution of 40 ms.

Basic functional and volume analysis

Image analysis was performed off-line using a standardized approach by two experienced cardiac radiologists with delineation of papillary muscles and trabeculations using thresholding (version 5.3.4cvi42, Circle Vascular Imaging, Canada). The global LV and RV function and volume analysis were performed using a short 3D module. The end of diastole and systole were determined automatically, based on the largest and smallest volume calculated per phase.

RV tissue tracking strain analysis

The degree of deformation was determined by a set of imaginary nodes placed on the mid-curve between the endo- and epicardial boundaries, and these boundaries were tracked by a pre-defined algorithm through the cardiac cycle. The basis of these algorithms has been previously described, and their validity has been demonstrated (11). The RV diastolic phase was determined by using the RV specific trajectory tool with the correction of readers. The tissue tracking analysis was performed by drawing out the long axis and the short axis endo- and epicardial border. The trabecula was carefully excluded, and the tricuspid plane and the apex were marked on the long axis and the short axis of the RV.

Myocardial strain was defined as the percentage of

Table 1 Patient characteristics

Variables	Female (n=60)	Male (n=60)	Overall (n=120)	P
Age (years)	47.3±17.2	44.5±16.6	46.0±14.8	0.053
Height (cm)	163.2±3.3	172.8±5.3	167.5±6.4	<0.001
Weight (kg)	60.2±7.4	73.8±11.5	66.4±11.6	0.002
BMI (kg/m^2)	22.6±2.6	24.7±3.3	23.6±3.1	0.372
LVEF (%)	69.0±7.9	68.8±7.2	69.0±7.5	0.25
LVEDVi (mL/m^2)	59.3±8.6	62.9±10.5	60.9±9.6	0.016
LVESVi (mL/m^2)	20.9±6.3	21.8±6.3	21.3±6.3	0.04
RVEF (%)	62.6±7.8	62.9±7.8	62.7±7.7	0.71
RVEDVi (mL/m^2)	52.3±6.9	59.5±12.5	55.6±10.4	<0.001
RVESVi (mL/m^2)	23.7±7.7	23.2±6.8	23.5±7.3	0.30

BMI, body mass index; LV, left ventricle; RV, right ventricle; EF, ejection fraction; EDVi, end-diastolic volume index; ESVi, end-systolic volume index.

myocardial fiber shortening at the end of contraction versus the end of diastole. The long axis stress was negative due to ventricular contraction; the myocardium at the latitude of the long axis was shortened. Both myocardial strain and strain rate parameters were obtained. Myocardial stress rate is defined as the changes in myocardial stress overtime. Myocardial stress and stress rate were measured in different directions: long axis, radial direction, and circumferential direction (12).

Differences between observers were analyzed by two researchers using RV motion pictures in 20 patients. The same images were analyzed by the operators, and the results were recorded independently for blind evaluation. Intra-observer variability was assessed by one observer at different points in the 7 to 10 days for 20 patients.

Statistical analysis

For standard distribution and continuous variables, the mean value ± standard deviation is used. Data analysis was performed by SPSS 22 software program. The Shapiro-Wilk test was used to test the standard degree. The independent sample t-test was used to compare gender differences. The sample size was set based on power analysis for the analysis of variance (ANOVA) testing between age and gender. An estimated mean difference of 10, alpha* values of 0.05, and a power of 95 were used (8). To test for significant differences between RV strain measurements in patient groups of different BMI and ages, analysis of variance (ANOVA) testing was performed. The distribution of continuous variables was evaluated by the Kolmogorov–Smirnov test. Differences between patients and controls were compared by unpaired t-test. Spearman's Rho-related tests were used to assess the relationship between stress and stress rate and age. Consistency was tested by Bland-Altman analysis, along with an intragroup correlation coefficient to calculate the 95% limits of mean deviation and consistency. P<0.05 was considered statistically significant.

Results

Patient characteristics

Following the strict inclusion criteria, 120 eligible volunteers (mean age 46.0±14.8 years, 50% men) were included in CMR scanning. The basic information of the subjects including the height, weight, body mass index (BMI), and ejection fraction (EF), end-diastolic volume (EDV) and end-systolic volume (ESV) of the LV and RV are shown in *Table 1*.

The intra- and inter-observer variability of our study is given in *Table 2*. In Bland–Altman analyses, the GLS had the best intra-observer agreement (–0.13±0.51; 95% CI, –1.13–0.87) and theGRS had the best interobserver agreement (0.054±0.31; 95% CI, –0.55–0.66). The time required to the post-process of RV tissue tracking was 5.4±2.7 min per participant.

Table 2 Intra-observer and inter-observer variability

Strain	Variability	Mean Bias ± SD	Limits of agreement	ICC
GRS	Intra-observer	–1.29±3.13	–7.42 to 4.84	0.97
	Inter-observer	0.054±0.31	–0.55 to 0.66	0.99
GLS	Intra-observer	–0.13±0.51	–1.13 to 0.87	0.99
	Inter-observer	0.47±2.76	–4.93 to 5.87	0.86
GCS	Intra-observer	0.25±0.78	–1.28 to 1.78	0.99
	Inter-observer	–0.38±2.43	–5.14 to 4.38	0.90

GRS, global peak radial strain; GLS, global peak longitudinal strain; GCS, global peak circumferential strain; ICC, intraclass correlation coefficient.

Table 3 Basic cardiac magnetic resonance (CMR) functional parameters by age decile (%)

Variables	Age deciles (n=24)					
	20–29 years	30–39 years	40–49 years	50–59 years	60–69 years	P
LVEF (%)	65±8	67±7	69±6	69±8	73±7	0.339
LVEDVi (mL/m^2)	65±9	65±9	60±11	60±8	57±7	0.220
LVESVi (mL/m^2)	23±7	22±4	21±5	21±7	20±7	0.562
RVEF (%)	61±7	62±7	64±7	61±6	67±9	0.246
RVEDVi (mL/m^2)	60±12	61±14	55±10	52±5	52±5	0.183
RVESVi (mL/m^2)	24±6	24±7	23±7	23±7	25±9	0.61

LV, left ventricle; RV, right ventricle; EF, ejection fraction; EDVi, end-diastolic volume index; ESVi, end-systolic volume index.

Normal references for CMR functional parameters

The functional parameters, including EF and indexed volumes of the LV and RV, are presented in *Table 1*. LV end-diastolic volume index (LVEDVi), LV end-systolic volume index (LVESVi) and RV end-diastolic volume index (RVEDVi) were significantly different between females and males (P<0.05 for all). The values for LVEF and RVEF were similar in males and females. There was no significant difference between different age groups in all LV and RV basic functional parameters (P>0.05 for all) (*Table 3* and *Table S1*).

Normal reference of RV strain using CMR-TT

Strain and strain rate of RV global and regional myocardium in healthy subjects of a Chinese population, and gender correlation, are shown in *Table 4* and *Table S2*. The global peak longitudinal strain (GLS) and global peak radial strain (GRS) was –24.3±4.7 and 23.0±8.5. The peak circumferential strains (GCS) for global, basal, mid-cavity and apical segments were –13.3±4.1, –13.1±4.0, –12.5±4.7, and –15.9±5.8, respectively. There were significant gender differences in peak GRS (P=0.009) and at the base (P=0.017) and the mid-cavity (P=0.011) with greater deformation in females than in males. However, there was no significant gender correlation at the peak GLS (P=0.056), peak longitudinal systolic strain rate (GLS S' P=0.178), and peak longitudinal systolic strain rate (GLS D' P=0.117). Moreover, there were also significant age differences in GRS (P<0.001) and GCS for basal (P<0.001) and the mid-cavity (P=0.037) segments, which increased with age to different degrees (*Table 5*) (*Figure 1*).

Correlation between RV peak strain and BMI in healthy subjects

The mean value of BMI was 23.6±3.1 kg/m^2. There was no correlation between BMI and the RVGLS (P=0.98), GRS (P=0.71), and GCS at the base, middle, and apex (P=0.87, P=0.60, P=0.28). Moreover, there was no significant

Table 4 Right ventricular (RV) strain and strain rate by cardiac magnetic resonance cine image-based tissue tracking technology (CMR-TT)

Variables	Female (n=60)	Male (n=60)	Overall (n=120)	P
GRS	24.9±8.7	20.7±7.7	23.0±8.5	0.009
GLS	−25.1±5.2	−23.4±3.8	−24.3±4.7	0.056
GCS	−14.2±4.1	−12.3±3.9	−13.3±4.1	0.014
GCS-b	−11.5±4.6	−14.2±4.4	−13.1±4.0	0.017
GCS-m	−13.5±4.7	−11.2±4.4	−12.5±4.7	0.011
GCS-a	−15.5±5.7	−16.4±5.9	−15.9±5.8	0.41
GRS S’	1.4±0.7	1.2±0.5	1.3±0.6	0.047
GCS S’	−0.8±0.3	−0.7±0.3	−0.8±0.3	0.27
GLS S’	−1.7±0.6	−1.5±0.6	−1.6±0.6	0.178
GRS D’	−1.4±0.5	−1.2±0.5	−1.3±0.5	0.026
GCS D’	0.8±0.2	0.7±0.2	0.7±0.2	0.027
GLS D’	1.3±0.3	1.4±0.4	1.3±0.4	0.117

GRS, global peak radial strain; GLS, global peak longitudinal strain; GCS, global peak circumferential strain; GCS-b, global peak circumferential strain for basal; GCS-m, global peak circumferential strain for mid; GCS-a, global peak circumferential strain for apical; GRS S’, peak radial systolic strain rate; GCS S’, peak circumferential systolic strain rate; GLS S’, peak longitudinal systolic strain rate; GRS D’, peak radial diastolic strain rate; GCS D’, peak circumferential diastolic strain rate; GLS D’, peak longitudinal diastolic strain rate.

Table 5 Right ventricular (RV) strain and strain rate by age decile (%)

Variables	Age deciles (N=24)					
	20–29 years	30–39 years	40–49 years	50–59 years	60–69 years	P
GRS	19.4±5.3	22.0±7.3	18.5±5.8	24.9±8.0	30.3±10.4	<0.001
GCS	−11.6±2.8	−12.8±4.0	−11,3±3.1	−14.1±3.6	−16.6±4.6	<0.001
GLS	−24.5±3.6	−23.7±4.9	−24.9±3.8	−23.1±7.0	−25.4±3.7	0.764
GCS-b	−12.40±2.83	−13.65±3.59	−11.30±3.87	−16.51±4.07	−17.07±5.42	<0.001
GCS-m	−11.64±3.52	−12.35±4.48	−10.61±4.03	−12.38±4.43	−15.35±5.11	0.037
GCS-a	−14.05±5.01	−16.27±5.78	−15.88±5.14	−15.97±4.97	−16.90±7.61	0.828
GRS S’	1.09±0.39	1.45±1.06	1.04±0.36	1.51±0.55	1.56±0.52	0.255
GCS S’	−0.67±0.22	−0.77±0.21	−0.64±0.22	−0.87±0.26	−0.86±0.30	0.054
GLS S’	−1.75±0.4.0	−1.41±0.91	−1.63±0.41	−1.45±0.83	−1.66±0.36	0.255
GRS D’	−1.20±0.42	−1.36±0.65	−0.93±0.35	−1.42±0.45	−1.56±0.60	0.02
GCS D’	0.74±0.21	0.72±0.21	0.60±0.17	0.79±0.20	0.74±0.24	0.018
GLS D’	1.41±0.43	1.37±0.37	1.19±0.28	1.36±0.39	1.24±0.26	0.847

GRS, global peak radial strain; GLS, global peak longitudinal strain; GCS, global peak circumferential strain; GCS-b, global peak circumferential strain for basal; GCS-m, global peak circumferential strain for mid; GCS-a, global peak circumferential strain for apical; GRS S’, peak radial systolic strain rate; GCS S’ peak circumferential systolic strain rate; GLS S’, peak longitudinal systolic strain rate; GRS D’, peak radial diastolic strain rate; GCS D’, peak circumferential diastolic strain rate; GLS D’, peak longitudinal diastolic strain rate.

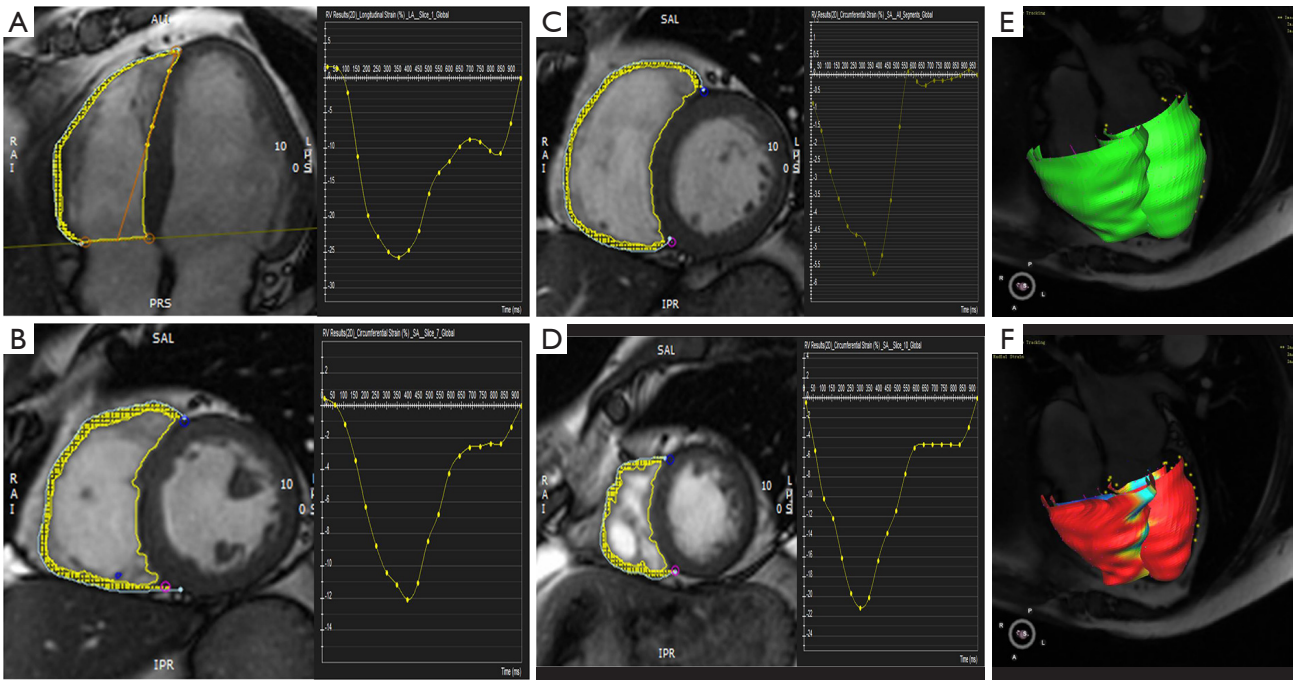

Figure 1 The cardiac magnetic resonance tissue tracking: (A) four-chamber long-axis strain, (B) the short axis circumferential basal strain, (C) short-axis circumferential mid strain, (D) short-axis circumferential apex strain. The A-D images are all diastolic images. Yellow is the tracking for the right ventricle. Each curve shows the strain values of the right ventricle in 25 phases, including the peak value. (E,F) 3D models of the right ventricle; E is diastole and F is systole.

correlation between BMI and peak radial systolic strain rate and peak radial diastolic strain rate (P=0.98, P=0.37) (*Table 6*).

Discussion

In this study, we reported the reference values for RV myocardial strain using CMR-TT from a group of healthy Chinese volunteers across a balanced stratification of age and sex. We also demonstrated an association between RV strain or strain rate parameters assessed by CMR-TT and either age or sex, and provide age-stratified normal range values for right heart CMR-TT. These results will have significant consequences for the prognostic stratification of congenital and acquired cardiovascular diseases, even though the relationship between baseline biventricular volumes and age were similar to that observed in the general population. The reproducibility of RV strain was also highly satisfactory. These findings suggest that CMR-TT is a novel technique which is fast, convenient, and can accurately assess both RV longitudinal and circumferential strain, while facilitating the rapid measurement of myocardial deformation without the limitation of the acoustic window or need for additional sequence acquisition.

Starting with the application of crystal sonomicrometry in dogs in the 1970s, the last decades have witnessed a surge in imaging techniques that can visualize local myocardial wall motion (deformation) (13). Tissue tagging, a CMR technique that prescribes multiple grids on the myocardial tissue to track deformation throughout the cardiac cycle, is typically regarded as the golden standard for LV deformation (14). Echocardiographic deformation imaging using either speckle tracking or tissue Doppler imaging has also gained popularity for those patients unfit to undergo CMR examinations (12,15). Of note, these techniques are technically demanding, time-consuming, and have primarily been validated for use in the LV, but render themselves less suitable for the thin-walled and highly trabeculated RV (11,16-20).

CMR-TT is a new method for CMR to evaluate myocardial strain using conventional CMR cine image, which can be easily acquired without contrast agent. With semi-auto contouring, the left and RV endocardium and epicardium at the end of diastole from conventional CMR cine image, myocardial tissue tracking strain, and strain

Table 6 Right ventricular (RV) strain and strain rate by BMI

Variables	BMI <18.5 (N=21)	18.5<BMI<23.9 (N=44)	24<BMI<27 (N=25)	28<BMI<32 (N=24)	P
GRS	27.13±3.32	22.10±7.19	24.42±9.36	21.50±11.13	0.711
GLS	−21.30±3.41	−24.18±5.13	−24.8±4.21	−24.11±4.55	0.987
GCS	−15.53±1.20	−12.70±3.41	−14.09±4.61	−12.80±5.28	0.42
GCS-b	−16.28±1.75	−13.57±4.01	−15.40±4.71	−12.52±5.01	0.869
GCS-m	−13.95±1.98	−12.29±4.12	−12.72±5.07	−11.95±6.35	0.599
GCS-a	−17.82±4.12	−14.86±5.51	−17.22±5.97	−16.08±6.36	0.278
GRS S’	1.41±0.10	1.21±0.46	1.50±0.83	1.18±0.56	0.978
GCS S’	−0.86±0.09	−0.72±0.23	−0.84±0.27	−0.71±0.29	0.383
GLS S’	−1.74±0.23	−1.67±0.65	−1.47±0.60	−1.60±0.39	0.567
GRS D’	−1.45±0.12	−1.21±0.42	−1.35±0.62	−1.22±0.63	0.373
GCS D’	0.83±0.04	0.72±0.19	0.70±0.23	0.67±0.25	0.584
GLS D’	1.28±0.24	1.34±0.40	1.32±0.30	1.30±0.35	0.991

GRS, global peak radial strain; GLS, global peak longitudinal strain; GCS, global peak circumferential strain; GCS-b, global peak circumferential strain for basal; GCS-m, global peak circumferential strain for mid; GCS-a, global peak circumferential strain for apical; GRS S’, peak radial systolic strain rate; GCS S’, peak circumferential systolic strain rate; GLS S’, peak longitudinal systolic strain rate; GRS D’, peak radial diastolic strain rate; GCS D’, peak circumferential diastolic strain rate; GLS D’, peak longitudinal diastolic strain rate.

rate were determined automatically (21). Compared with ultrasound speckle tracking imaging technology, CMR-TT is not affected by imaging angle, can directly observe morphological changes of the ventricle, and obtain two-ventricular free wall myocardial strain (22-26). In conditions leading to RV pressure or volume overloads such as pulmonary hypertension, tetralogy of Fallot, or Systemic RV, the contractile pattern changes from longitudinal to circumferential shortening (27,28). Given this, RV circumferential strain is also critical for those patients in clinical practice. Our study shows that CMR-TT provides highly reproducible information on RV myocardial motion not only in the longitudinal but also in the circumferential direction. CMR-TT is a fast and easy to operate non-invasive imaging technology that produces three-dimensional detailed anatomical images without the use of ionizing radiation at an average post-processing time 5 of minutes; these characteristics can overcome some limitations of echocardiography such as the ability to reproducibly visualize the entire R.

Moreover, the CMR-TT software we used in this study provides a dedicated RV strain analysis tool, which speeds up our study workflow and yields more objective results. RV TT method computes the strain with gradient optical flow algorithm, which can be very sensitive to morphologic changes affecting RV endocardial or epicardial borders. We have provided segmental GCS reference ranges based on the apex, mid and basal segments of the RV since the previous study has demonstrated that most basal and mid-ventricular segments have good reproducibility, but at the apex, reproducibility is poor. This effect is likely due to the thinning of the ventricular wall and increased blurring of the endocardium-blood pool boundary.

Truong *et al.* (29) demonstrated that global RV longitudinal strain peak had a correlation with gender in 50 healthy volunteers, with a GLS of −22.11%±3.51%. The GCS for global, basal, mid-cavity, and apical segments follow respectively: −11.69%±2.25%, −11.00%±2.45%, −11.17%±3.36%, and −12.90%±3.34%. Liu *et al.* (30) reported the normal parameters of the RV long axis in 100 normal volunteers from the cardiovascular research center of the University of Birmingham, UK, and found the RV longitudinal strain was -24.2%±3.59%, and the peak systolic strain rate was −1.54±0.41 s^{-1}. However, the myocardial strain rate and age differences were not involved in this study. In our study, we analyzed the normal reference of RV myocardial strain parameters using CMR-TT technology with a larger Chinese cohort. The GLS and GRS was −24.3±4.7 and 23.0±8.5. The GCS for global, basal, mid-cavity, and apical segments were −13.1±4.0, −12.5±4.7 and

–15.9±5.8, respectively, which were slightly greater than the previous study. For both the left and RV, our findings exhibited greater EF and volumes that were higher with advancing age in both genders, which is consistent with the previous study from the UK (27). Their study showed a small increase from age 50 years between strain and strain rate. However, the age differences in EF and volume were not statistically significant in our study. The RV global and regional strain and the strain rate of the female subjects were both greater than the male subjects. The values of RV longitudinal strain and mid and basal circumferential strain grew slightly with the age increase. Our study included a larger cohort of 120 healthy subjects from each decade of life between 20 and 70 without known congenital or acquired cardiovascular disease, hypertension, diabetes, dyslipidemia, or systemic inflammatory disorders, and who underwent cardiac magnetic resonance tissue tracking (CMR-TT) assessment of RV myocardial strain and strain rate. The normal reference of the Chinese population was consistent with these two previous studies. There were also significant age and gender differences in GRS and GCS for the basal and mid-cavity segments; however, there was no difference in peak GLS, which is considered an early myocardial dysfunction parameter in most cardiac and pulmonary artery disease.

The results from our data also show that the intra-and inter-observer variability was further improved in terms of repeatability with dedicated trained radiologists. Due to significant variations in strain values obtained by different software solutions and measurement techniques, to date, these new parameters should be quantified similarly if serial assessments or follow-up acquisitions are required. Similar problems have been successfully addressed in echocardiographic speckle-tracking with efforts being directed towards consensus (31) and trying to standardize technology to enable wider interchangeability and comparisons. Therefore, more clinical trials are needed, and the technical and software specific properties in CMR imaging need to be evaluated to reliably introduce standardization and reference values for myocardial deformation assessment for widespread clinical introduction.

This study has some limitations. This is a prospective study with a limited cohort from one center. No comparison was performed between CMR-TT with myocardial tagging, SENC, or DENSE, as those sequences were not available at the time of examination. However, this data is comprehensive, advanced, and accurate, and has high clinical practicability. Furthermore, CMR examinations were not performed repeatedly on the same individuals over time. Therefore, the associations described between age and CMR parameters are not longitudinal, but instead cross-sectional. It is believed that with more research focusing on RV dysfunction and novel techniques with a promising new strain algorithm designed to handle motion discontinuities properly, this technology will be applied widely to patients with various RV diseases.

In summary, the age- and gender-related normal references of RV strain values were provided by CMR-TT using the SSFP sequence in 120 healthy Chinese volunteers with a wide age range separated by sex. These reference values can be applied widely to evaluate early myocardial dysfunction in patients with suspected RV disease, especially for Chinese populations.

Acknowledgments

Funding: This study was funded by the National Nature Science Foundation of China (81871435).

Footnote

Conflicts of Interest: The authors have no conflicts of interest to declare.

Ethical Statement: This study was approved by Ethics Review Board of First Affiliated Hospital of China Medical University.

References

1. Ballo P, Fibbi V, Granelli M, Fusco F, Abbondanti A, Fantini A, Bartalini M, Consalvo M, Fazi A, Santoro GM. Giant isolated intracardiac thrombus presenting as acute heart failure secondary to right ventricular outflow tract obstruction in a patient with renal carcinoma. Oxf Med Case Reports 2018;2018:omy019.
2. Sugamoto K, Kurishima C, Iwamoto Y, Ishido H, Masutani S, Ushinohama H, Sagawa K, Ishikawa S, Nakano T, Kado H, Senzaki H. Cardiac Ventricular Contractile Responses to Chronically Increased Afterload Secondary to Right Ventricular Outflow Obstruction in Patients With Tetralogy of Fallot. Am J Cardiol 2018;121:1090-3.
3. Hanboly NH, Baghdady YM, Diab RH, Lawend SR, Kenawy AA. Value of three-dimensional echocardiography study of left ventricle function correlated to coronary arterial dominance in predicting the outcome of primary

percutaneous coronary intervention. J Saudi Heart Assoc 2018,30:211-21.
4. Mavrakanas TA, Khattak A, Singh K, Charytan DM. Echocardiographic parameters and renal outcomes in patients with preserved renal function, and mild- moderate CKD. BMC Nephrol 2018;19:176.
5. Mondal P, Kumar P, Vinayak M, Passi A, Sinha DP. Assessment of Right Ventricular Function by Newer Imaging in Echocardiography in Idiopathic Pulmonary Arterial Hypertension. Cardiol Res 2017,8:214-9.
6. Bourfiss M, Vigneault DM, Aliyari Ghasebeh M, Murray B, James CA, Tichnell C, Mohamed Hoesein FA, Zimmerman SL, Kamel IR, Calkins H, Tandri H, Velthuis BK, Bluemke DA, Te Riele ASJM. Feature tracking CMR reveals abnormal strain in preclinical arrhythmogenic right ventricular dysplasia/ cardiomyopathy: a multisoftware feasibility and clinical implementation study. J Cardiovasc Magn Reson 2017;19:66.
7. Buckert D, Witzel S, Steinacker JM, Rottbauer W, Bernhardt P. Comparing Cardiac Magnetic Resonance-Guided Versus Angiography-Guided Treatment of Patients With Stable Coronary Artery Disease: Results From a Prospective Randomized Controlled Trial. JACC Cardiovasc Imaging 2018;11:987-96.
8. Andre F, Steen H, Matheis P, Westkott M, Breuninger K, Sander Y, Kammerer R,Galuschky C, Giannitsis E,Korosoglou G, Katus HA, Buss SJ. Age- and gender-related normal left ventricular deformation assessed by cardiovascular magnetic resonance feature tracking. J Cardiovasc Magn Reson 2015;17:25.
9. Cao JJ, Ngai N, Duncanson L, Cheng J, Gliganic K, Chen Q. A comparison of both DENSE and feature trackingtechniques with tagging for the cardiovascular magnetic resonance assessment of myocardial strain. J Cardiovasc Magn Reson 2018;20:26.
10. Amzulescu MS, Langet H, Saloux E, Manrique A, Boileau L, Slimani A, Allain P, Roy C, de Meester C, Pasquet A, De Craene M, Vancraeynest D, Pouleur AC, Vanoverschelde JJ, Gerber BL. Head-to-Head Comparison of Global and Regional Two-Dimensional Speckle Tracking Strain Versus Cardiac Magnetic Resonance Tagging in a Multicenter Validation Study. Circ Cardiovasc Imaging 2017;10. doi: 10.1161/CIRCIMAGING.117.006530.
11. Agabiti-Rosei E, Muiesan ML, Salvetti M. Evaluation of subclinical target organ damage for risk assessment and treatment in the hypertensive patients: left ventricular hypertrophy. J Am Soc Nephrol 2006;17:S104-8.
12. Azak E, Cetin II, Gursu HA, Kibar AE, Surucu M, Orqun A, Pamuk U. Recovery of myocardial mechanics in Kawasaki disease demonstrated by speckle tracking and tissue Doppler methods. Echocardiography 2018;35:380-7.
13. Carlsson E, Milne EN. Permanent implantation of endocardial tantalum screws: a new technique for functional studies of the heart in the experimental animal. J Can Assoc Radiol 1967;18:304-9.
14. Wu L, Germans T, Guclu A, Heymans MW, Allaart CP, van Rossum AC. Feature tracking compared with tissue tagging measurements of segmental strain by cardiovascular magnetic resonance. J Cardiovasc Magn Reson 2014;16:10.
15. Roshdy HS, El-Dosouky II, Soliman MH. High-risk inferior myocardial infarction: Can speckle tracking predict proximal right coronary lesions? Clin Cardiol 2018;41:104-10.
16. Chen J, Yang ZG, Xu HY, Shi K, Guo YK. Assessment of left ventricular myocardial deformation by cardiac MRI strain imaging reveals myocardial dysfunction in patients with primary cardiac tumors. Int J Cardiol 2018;253:176-82.
17. Santarelli G, Lopez JT, Del Palacio JF. Effects of a combination of acepromazine maleate and but orphanol tartrate on conventional and two-dimensional speckle tracking echocardiography in healthy dogs. Am J Vet Res 2017;78:158-67.
18. Tong X, Poon J, Li A, Kit C, Yamada A, Shiino K, Ling LF, Choe YH, Chan J, Lau YK, Ng MY. Validation of cardiac magnetic resonance tissue tracking in the rapid assessment of RV function: a comparative study to echocardiography. Clin Radiol 2018;73:324.e9-324.e18.
19. Rai AB, Lima E, Munir F, Faisal Khan A, Waqas A, Bughio S, ul Haq E, Attique HB, Rahman ZU. Speckle Tracking Echocardiography of the Right Atrium: The Neglected Chamber. Clin Cardiol 2015;38:692-7.
20. Brandimarte C, Battista M, Galie M, Delfino M. Thoracic pain and myocardial ischemia. Applications of the Bayestheorem for the rational use of stress-test including echocardiography-dobutamine. Recenti Prog Med 1996;87:564-70.
21. Hor KN, Baumann R, Pedrizzetti G, Tonti G, Gottliebson WM, Taylor M, Benson DW, Mazur W. Magnetic resonance derived myocardial strain assessment using feature tracking. J Vis Exp 2011;(48). doi: 10.3791/2356.
22. Kashioulis P, Lundgren J, Shubbar E, Nguy L, Saeed A, Guron CW, Guron G. Adenine-Induced Chronic Renal Failure in Rats: A Model of Chronic Renocardiac Syndrome with Left Ventricular Diastolic Dysfunction but Preserved Ejection Fraction. Kidney Blood Press Res

2018;43:1053-64.
23. Dungen HD, Petroni R, Correale M, Coiro S, Monitillo F, Triggiani M, Leone M, Antohi EL, Ishihara S, Sarwar CMS, Sabbah HN, Memo M, Metra M, Butler J, Nodari S, Gheorghiade M. A new educational program in heart failure drug development: the Brescia international master program. J Cardiovasc Med (Hagerstown) 2018;19:411-21.
24. Patel YR, Robbins JM, Kurgansky KE, Imran T, Orkaby AR, Mclean RR, Ho YL, Cho K, Michael Gaziano J, Djousse L, Gagnon DR, Joseph J. Development and validation of a heart failure with preserved ejection fraction cohort using electronic medical records. BMC Cardiovasc Disord 2018;18:128.
25. Pi SH, Kim SM, Choi JO, Kim EK, Chang SA, Choe YH, Lee SC, Jeon ES. Prognostic value of myocardial strain and late gadolinium enhancement on cardiovascular magnetic resonance imaging in patients with idiopathic dilated cardiomyopathy with moderate to severely reduced ejection fraction. J Cardiovasc Magn Reson 2018;20:36.
26. Senthilnathan M, Kundra P, Mishra SK, Velayudhan S, Pillai AA. Competence of Intensivists in Focused Transthoracic Echocardiography in Intensive Care Unit: A Prospective Observational Study. Indian J Crit Care Med 2018,22:340-5.
27. Sljivic A, Pavlovic Kleut M, Bukumiric Z, Celic V. Association between right ventricle two- and three-dimensional echocardiography and exercise capacity in patients with reduced left ventricular ejection fraction. PLoS One 2018;13:e0199439.
28. Park JH, Choi JO, Park SW, Cho GY, Oh JK, Lee JH, Seong IW. Normal references of right ventricular strain values by two-dimensional strain echocardiography according to the age and gender. Int J Cardiovasc Imaging 2018,34:177-83.
29. Truong VT, Safdar KS, Kalra DK, Gao X, Ambach S, Taylor MD, Moore R, Taylor RJ, Germann J. Cardiac magnetic resonance tissue tracking in right ventricle: Feasibility and normal values. Magn Reson Imaging 2017;38:189-95.
30. Liu B, Dardeer AM, Moody WE, Edwards NC, Hudsmith LE, Steeds RP. Normal values for myocardial deformation within the right heart measured by feature-tracking cardiovascular magnetic resonance imaging. Int J Cardiol 2018;252:220-3.
31. Voigt JU, Pedrizzetti G, Lysyansky P, Marwick TH, Houle H, Baumann R. Definitions for a common standard for 2D speckle tracking echocardiography: consensus document of the EACVI/ASE/Industry Task Force to standardize deformation imaging. Eur Heart J Cardiovasc Imaging 2015;16:1-11.

Cite this article as: Liu T, Wang C, Li S, Zhao Y, Li P. Age- and gender-related normal references of right ventricular strain values by tissue tracking cardiac magnetic resonance: results from a Chinese population. Quant Imaging Med Surg 2019;9(8):1441-1450. doi: 10.21037/qims.2019.08.13

Supplementary

Table S1 Cardiac basic function and right ventricular (RV) strain by age and gender

Variables	Gender	Age deciles					
		20–29 years	30–39 years	40–49 years	50–59 years	60–69 years	P
LVEF (%)	Male (N=12)	65.8±8.7	68.0±8.3	68.7±5.6	69.6±7.6	72.1±3.2	0.695
	Female (N=12)	65.0±8.1	66.6±5.3	69.6±6.8	68.2±9.1	74.1±8.0	0.699
RVEF (%)	Male (N=12)	62.3±7.1	63.4±8.0	62.4±6.1	62.2±5.2	69.9±9.9	0.376
	Female (N=12)	59.6±7.7	60.1±6.5	64.3±7.7	60.8±6.5	65.8±9.2	0.377
GRS	Male (N=12)	19.8±6.9	19.9±6.5	17.3±5.9	22.4±6.8	26.9±10.0	0.027
	Female (N=12)	18.9±2.7	24.5±7.7	19.3±5.8	26.2±8.5	32.1±10.5	0.031
GLS	Male (N=12)	–22.7±2.7	–23.3±4.3	–24.7±3.6	–22.6±5.0	–23.8±4.8	0.083
	Female (N=12)	–26.5±3.6	–24.1±5.7	–24.9±4.0	–23.4±8.1	–26.3±2.8	0.093
GCS	Male (N=12)	–112±3.4	–12.0±3.6	–10.8±3.2	–13.3±3.0	–15.1±4.5	0.033
	Female (N=12)	–11.9±1.6	–13.7±4.3	–11.6±3.1	–14.4±3.8	–17.4±4.5	0.036

LV, left ventricle; RV, right ventricle; EF, ejection fraction; GRS, global peak radial strain; GLS, global peak longitudinal strain; GCS, global peak circumferential strain.

Table S2 Right ventricular (RV) strain rate by age and gender

Variables	Gender	Age deciles					
		20–29 years	30–39 years	40–49 years	50–59 years	60–69 years	P
GRS S’	Male (N=12)	1.1±0.4	1.2±0.4	0.9±0.3	1.3±0.3	1.4±0.5	0.076
	Female (N=12)	0.9±0.2	1.7±1.4	1.1±0.3	1.6±0.6	1.6±0.5	0.094
GLS S’	Male (N=12)	–1.6±0.3	–1.3±1.2	–1.4±0.2	–1.5±0.3	–1.4±0.2	0.169
	Female (N=12)	–1.8±0.3	–1.5±0.2	–1.7±0.4	–1.3±1.0	1.7±0.3	0.164
GCS S’	Male (N=12)	–0.7±0.2	–0.7±0.2	–0.5±0.2	–0.8±0.2	–0.8±0.3	0.442
	Female (N=12)	–0.6±0.1	–0.8±0.1	–0.6±0.2	–0.9±0.3	–1.6±0.6	0.444
GRS D’	Male (N=12)	–1.2±0.1	–1.2±0.5	–0.8±0.2	–1.3±0.4	–1.4±0.6	0.097
	Female (N=12)	–1.2±0.2	–1.5±0.7	–1.0±0.4	–1.5±0.5	–1.6±0.6	0.102
GLS D’	Male (N=12)	1.5±0.4	1.4±0.4	1.1±0.2	1.5±0.6	1.2±0.2	0.182
	Female (N=12)	1.3±0.3	1.2±0.2	1.2±0.3	1.3±0.3	1.2±0.3	0.163
GCS D’	Male (N=12)	0.7±0.2	0.7±0.2	0.5±0.1	0.7±0.2	0.7±0.3	0.147
	Female (N=12)	0.7±0.2	0.7±0.1	0.6±0.2	0.8±0.2	0.8±0.2	0.137

GCS S’, peak circumferential systolic strain rate; GLS S’, peak longitudinal systolic strain rate; GRS D’, peak radial diastolic strain rate; GCS D’, peak circumferential diastolic strain rate; GLS D’, peak longitudinal diastolic strain rate.